



Since January 2020 Elsevier has created a COVID-19 resource centre with free information in English and Mandarin on the novel coronavirus COVID-19. The COVID-19 resource centre is hosted on Elsevier Connect, the company's public news and information website.

Elsevier hereby grants permission to make all its COVID-19-related research that is available on the COVID-19 resource centre - including this research content - immediately available in PubMed Central and other publicly funded repositories, such as the WHO COVID database with rights for unrestricted research re-use and analyses in any form or by any means with acknowledgement of the original source. These permissions are granted for free by Elsevier for as long as the COVID-19 resource centre remains active.



# Human choice to self-isolate in the face of the COVID-19 pandemic: A game dynamic modelling approach



Calistus N. Ngonghala<sup>a,b</sup>, Palak Goel<sup>c</sup>, Daniel Kutor<sup>a</sup>, Samit Bhattacharyya<sup>c,\*</sup>

<sup>a</sup> Department of Mathematics, University of Florida, Gainesville, FL 32611, USA

<sup>b</sup> Emerging pathogens Institute, University of Florida, Gainesville, FL 32610, USA

<sup>c</sup> Disease Modelling Lab, Department of Mathematics, School of Natural Sciences, Shiv Nadar University, UP 201314, India

## ARTICLE INFO

### Article history:

Received 13 October 2020

Revised 14 March 2021

Accepted 17 March 2021

Available online 23 March 2021

### Keywords:

SARS-CoV-2

Social-distancing

Isolation

Quarantine

Human behavior

Evolutionary game theory

## ABSTRACT

Non-pharmaceutical interventions (NPIs) involving social-isolation strategies such as self-quarantine (SQ) and social-distancing (SD) are useful in controlling the spread of infections that are transmitted through human-to-human contacts, e.g., respiratory diseases such as COVID-19. In the absence of a safe and effective cure or vaccine during the first ten months of the COVID-19 pandemic, countries around the world implemented these social-isolation strategies and other NPIs to reduce COVID-19 transmission. But, individual and public perception play a crucial role in the success of any social-isolation measure. Thus, in spite of governments' initiatives to use NPIs to combat COVID-19 in many countries around the world, individual choices rendered social-isolation unsuccessful in some of these countries. This resulted in huge outbreaks that imposed a substantial morbidity, mortality, hospitalization, economic, etc., toll on human lives. In particular, human choices pose serious challenges to public health strategic decision-making in controlling the COVID-19 pandemic. To unravel the impact of this behavioral response to social-isolation on the burden of the COVID-19 pandemic, we develop a model framework that integrates COVID-19 transmission dynamics with a multi-strategy evolutionary game approach of individual decision-making. We use this integrated framework to characterize the evolution of human choices in social-isolation as the disease progresses and public health control measures such as mandatory lockdowns are implemented. Analysis of the model illustrates that SD plays a major role in reducing the burden of the disease compared to SQ. Parameter estimation using COVID-19 incidence data, as well as different lockdown data sets from India, and scenario analysis involving a combination of *Voluntary-Mandatory* implementation of SQ and SD shows that the effectiveness of this approach depends on the type of isolation, and the time and period of implementation of the selected isolation measure during the outbreak.

© 2021 Elsevier Ltd. All rights reserved.

## 1. Introduction

The end of 2019 was marked by the emergence of an unprecedented severe respiratory infection, COVID-19. COVID-19 is caused by a new member of the family of coronaviruses (SARS-CoV-2) that is related to the SARS (Severe Acute Respiratory Syndrome) and MERS (Middle Eastern Respiratory Syndrome) (Yin and Wunderink, 2018; World Health Organization, 2020). The spread of the virus worldwide has been rapid, with more than 32 million infections and 980,000 COVID-19 deaths within the first 9 months (i.e., from December to August, 2020). Among the countries hit the most by COVID-19 pandemic as of September 2020 were the Uni-

ted States of America (with over 7.1 million confirmed cases and 205,000 deaths), India (with over 5.7 million confirmed cases and 92,000 deaths), and Brazil (with over 4.5 million confirmed cases and 137,000 deaths) (Dong et al., 2020; World Health Organization, 2020). Although case numbers have been declining in some parts of the world, these staggering statistics indicate that the COVID-19 pandemic is still a major health problem to many parts of the world, especially since some countries are still experiencing exponential growth in the number of cases or a second wave of the pandemic (Routley, 2020). Hence, it is important to understand the transmission dynamics of the virus and the potential impact of various control and mitigation strategies in relation to human behavior and adaptation during the pandemic.

As of mid September 2020, there was no effective drug or vaccine for COVID-19. Thus, the only prevention or control measures

\* Corresponding author.

E-mail address: [samit.b@snu.edu.in](mailto:samit.b@snu.edu.in) (S. Bhattacharyya).

have been basic public health or non-pharmaceutical interventions (NPIs) including social-isolation such as self-quarantine (SQ) of suspected cases, e.g., requiring individuals who are suspected to have been in contact with a confirmed COVID-19 case or exposed to COVID-19 to stay away from others at home or in designated facilities; and social-distancing (SD), e.g., shelter-in-place, community lockdowns, closure of schools and non-essential businesses, avoiding crowded gatherings, staying about six feet apart in public, isolation (self and community) of confirmed cases, evacuation, etc. Many countries already went through a strict lockdown phase between March and May 2020, which contributed in reducing disease burden and pressure on healthcare systems. Some of these countries, e.g., China, Italy, Germany, Spain, etc., managed to keep their disease numbers low, as they started re-opening their economies after the first pandemic wave, while others, e.g., India, Mexico, Russia, etc., were experiencing a surge in the number of cases in the midst of re-opening (Gettleman, 2020). Irrespective of the control measure that a country adopted, individual and collective response to the measure, as well as timing of the measure was important in disease containment.

Since the emergence of the virus from China, one research direction has focused on the effective management and control of transmission. This has been approached in different ways including mathematical modelling. Specifically, many mathematical and computational models have been developed and used to 1) understand the potential magnitude of the epidemic, 2) determine key factors that characterize the severity of the outbreak, and 3) assess the impact of NPIs such as quarantine, SD, contact-tracing, face-mask use, etc., on the spread and burden of the virus (Flaxman et al., 2020; Gumel et al., 2021; Ngonghala et al., 2020a,b). Ferguson et al. (2020) assessed the impact of NPIs on COVID-19 through an agent-based framework, while Ngonghala et al. (2020) developed and used a deterministic model to investigate the impact of NPIs on the burden of COVID-19 (quantified in terms of hospitalizations and mortalities). The Institute for Health Metrics and Evaluation (2020) used a model to project the number of COVID-19-related mortalities in the entire US. Maier and Brockmann (2020) observed that there was a robust sub-exponential rise in the number of confirmed cases in Hubei province of China according to a scaling law during the transient episode of the epidemic. Tuite et al. (2020) used an age-structured compartmental model to study COVID-19 transmission in the population of Ontario, Canada. They investigated the impact of different lockdown durations on the dynamics of COVID-19. Some mathematical models including those by Ngonghala et al. (2020a,b) and Dickens et al. (2020) demonstrated that late implementation and premature relaxation of lockdown measures may trigger a resurgence of COVID-19 with a more devastating impact. Some studies including those in Gumel et al. (2021), Iboi et al. (2020) have studied the combined impact of an imperfect vaccine and NPIs such as SD and face mask use in public on COVID-19, while others have focused on the spatio-temporal spread of COVID-19. In particular, spatio-temporal research on COVID-19 includes studies aimed at understanding the effects of temperature on the early evolution of COVID-19 in Spain (Briz-Redón and Serrano-Aroca, 2020) and China (Xie and Zhu, 2020; Shi et al., 2020), the spatial dynamics of COVID-19 outbreak in China, USA, and some European communities, (Kang et al., 2020; Karaye and Horney, 2020; Mollalo et al., 2020), as well as predicting the spread of COVID-19 in Italy (Gatto et al., 2020; Martellucci et al., 2020; Giuliani et al., 2020).

Despite this theoretical elegance, very little research has focused on the impact of human behavior in response to social-isolation on the burden of the COVID-19 pandemic. Most of the recent technical reports and papers discuss social distancing behavior and optimal policy response to the COVID-19 pandemic

from several different foci (Alvarez et al., 2020; Chudik et al., 2020; Gonzalez-Eiras and Niepelt, 2020; Jones et al., 2020; Pindyck, 2020; Brotherhood et al., 2020; Toxvaerd, 2020). Others compare purely selfish and impure altruistic private versus social cost of contacts with heterogeneous age groups of healthy individuals (Acemoglu et al., 2020; Farboodi et al., 2020). In most cases, these studies use homogeneous SIR models to show how infected individuals internalise the part of the infection externality due to different altruistic preferences, or to what extent altruistic motives narrow the gap between selfish and socially optimal behavior. However, less research has focused on the evolution of SD or SQ behavior as the pandemic progresses, especially in face of intermittent mandatory lockdown approaches implemented by public health authorities in different countries. This represents a missed opportunity to advance a better understanding of interactions between the health, social, and economic burden of the pandemic from an individual and community decision-making perspective— aspects which could lead to the design and implementation of better disease mitigation measures. The risk–benefit profile of SD, for example, depends on the cost of SD and the probability that an individual is infected and becomes sick. Under a voluntary or poorly enforced mandatory policy, these costs may destabilize the effect of social-isolation. To date, approaches in most studies assessing the effect of social-isolation on COVID-19 control are *ad hoc* and do not take these individual-versus-group based risk–benefit dynamics into account. The ability to predict how risk–benefit profiles evolve will furnish public health authorities with improved evidence-based decision-making abilities and enable them to opt for an earlier switch to other control strategies or to implement a mixed policy within a given time frame.

This study attempts to understand the impact of the public perception of humans to adhere to the control measures implemented by governments to curtail the COVID-19 pandemic. In particular, we develop an integrated epidemiological-game dynamic model framework that couples the epidemiological characteristics of COVID-19 and human behavior in choosing specific NPIs, and parameterize the model with COVID-19 and social-isolation data from India to: 1) assess the impact of personal decision to adopt SQ or SD, and how these depend on different disease risk profiles, and to some extent, public health communication through the media, 2) investigate the impact and social costs associated with different mitigation strategies in reducing disease incidence, and 3) compare the impacts of voluntary and mandatory involvement in SQ and SD, and whether a combination of *voluntary-mandatory* approaches is better to contain the disease in the community.

## 2. Materials and methods

### 2.1. The epidemiological model

#### 2.1.1. Model derivation

The epidemiological model we consider here (see Fig. 1 for a conceptual framework) is a slightly modified version of the model in Ngonghala et al. (2020). The model splits humans into eight disjoint compartments representing quarantine and disease status. These are the class of: susceptible humans  $S$ , exposed humans  $E$ , infectious humans  $I$ , and recovered humans,  $R$ . The susceptible and exposed populations are further subdivided into non-quarantined and quarantined susceptible humans denoted by  $S_u$  and  $S_q$ , respectively, and non-quarantined and quarantined exposed humans denoted by  $E_u$  and  $E_q$ , respectively. It should be mentioned that quarantine can either be at home (SQ) or at a designated facility, although in the context of this study we are focusing on SQ. The infectious human population is also subdivided into infectious asymptomatic humans (those who transmit the virus

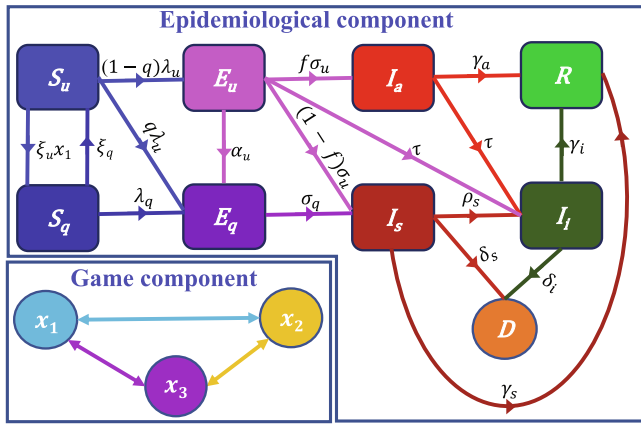


**Fig. 1.** Schematics for the model system (1) showing the flow of humans between different classes. The human population is subdivided in non-quarantined susceptible  $S_u$ , quarantined susceptible  $S_q$ , non-quarantined exposed  $E_u$ , quarantined exposed  $E_q$ , asymptomatic infectious  $I_a$ , (mild, severe, or critical) symptomatic infectious  $I_s$ , isolated (self or mandatory)  $I_i$ , and Recovered  $R$ . Parameters for the epidemiological component of the model are described in the text. For the behavior component of the model,  $x_1$  is the proportion of non-quarantined susceptible humans who choose to self-quarantine (SQ),  $x_2$  the fraction of non-quarantined susceptible humans who choose social-distancing (SD), and  $x_3 = 1 - (x_1 + x_2)$  is the proportion of non-quarantined susceptible humans who choose neither SQ nor SD.

without showing symptoms after the incubation period) denoted by  $I_a$ , infectious symptomatic humans  $I_s$  (clinically ill individuals, i.e., individuals who exhibit disease symptoms after the incubation period), and isolated infectious humans (identified symptomatic humans who are self-isolating or who have been placed in isolation in a health care facility denoted by  $I_i$ . The total human population at time  $t$ , is  $N(t) = S_u(t) + S_q(t) + E_u(t) + E_q(t) + I_a(t) + I_s(t) + I_i(t) + R(t)$ . To keep track of the number of COVID-19 related deaths, we use an additional class denoted by  $D$ .

Flow from the non-quarantined susceptible to the quarantined susceptible class is at rate  $\xi_u x_1$ , where  $x_1$  is the proportion of non-quarantined susceptible humans who choose to SQ at time  $t$ , while quarantined susceptible humans revert to the non-quarantined susceptible class at per capita rate  $\xi_q$  ( $1/\xi_q$  is the average duration of quarantine). Transition from the non-quarantined and quarantined susceptible classes ( $S_u$  and  $S_q$ ) to the exposed classes ( $E_u$  and  $E_q$ ) are through the forces of infection

$$\lambda_u = (1 - \epsilon x_2) \frac{\beta_a I_a + \beta_s (I_s + \eta_i I_i)}{N - \omega_q (S_q + E_q)}, \quad \lambda_q = \phi_q \frac{\beta_a I_a + \beta_s (I_s + \eta_i I_i)}{N - \omega_q (S_q + E_q)}$$

respectively, where  $0 \leq \epsilon \leq 1$  is the efficacy per day of SD in reducing disease transmission,  $0 \leq x_2 \leq 1$  denotes the fraction of non-quarantined susceptible humans who choose SD at time  $t$ ,  $0 < \eta_i < 1$  is the reduction in transmission by isolated humans,  $\beta_a$  is the effective contact rate with asymptomatic humans,  $\beta_s$  is the effective contact rate with symptomatic humans,  $0 \leq \omega_q \leq 1$  measures how effective quarantine is in preventing disease spread by quarantined humans, and  $1 - \phi_q$  ( $0 \leq \phi_q \leq 1$ ) is the efficacy of quarantine in preventing quarantined susceptible humans from being infected. In the context of this work, SD is broadly interpreted to include shelter-in-place, lockdown, closure of schools and non-essential businesses, avoiding crowds, maintaining a distance of six feet from others in public, etc., while SQ involves quarantine at home.

A proportion  $1 - q$  of the new infections join the exposed non-quarantined class, while the other proportion  $q$ , join the quarantined exposed class ( $q$  is the proportion of newly infected humans who are quarantined at the time of exposure). Non-quarantined exposed humans are either quarantined at rate  $\alpha_u$ , progress to

the infectious asymptomatic class at rate  $f\sigma_u$  after the incubation period ( $\sigma_u$  is the average incubation period for non-quarantined humans), or develop clinical COVID-19 symptoms at rate  $(1 - f)\sigma_u$  after the incubation period, where  $f$  is the fraction of non-quarantined exposed humans, who do not develop clinical disease symptoms after the incubation period. Non-quarantined exposed humans detected through diagnostic testing join the isolated infectious class at rate  $\tau$ . Quarantined exposed humans develop disease symptoms at rate  $\sigma_q$  after the incubation period ( $\sigma_q$  is the average incubation period for quarantined humans). Infectious asymptomatic humans are either detected (through diagnostic testing) and isolated at per capita rate  $\tau$  or recover at per capita rate  $\gamma_a$  ( $1/\gamma_a$  is the average duration of infection in asymptomatic humans), while infectious symptomatic humans are either isolated at per capita rate  $\rho_s$ , recover at per capita rate  $\gamma_s$  ( $1/\gamma_s$  is the average duration of infection in symptomatic humans), or die from COVID-19 at per capita rate  $\delta_s$ . Isolated humans either recover from infection at per capita rate  $\gamma_i$  or die from COVID-19 at per capita rate  $\delta_i$ .

Based on the conceptual framework presented in Fig. 1 and the state-variable and parameter descriptions, the epidemiological model is given by the system of differential equations:

$$\begin{aligned} \dot{S}_u &= \xi_q S_q - (\lambda_u + \xi_u x_1) S_u, \\ \dot{S}_q &= \xi_u x_1 S_u - (\lambda_q + \xi_q) S_q, \\ \dot{E}_u &= (1 - q)\lambda_u S_u - (\alpha_u + \sigma_u + \tau) E_u, \\ \dot{E}_q &= q\lambda_u S_u + \lambda_q S_q + \alpha_u E_u - \sigma_q E_q, \\ \dot{I}_a &= f\sigma_u E_u - (\gamma_a + \tau) I_a, \\ \dot{I}_s &= (1 - f)\sigma_u E_u + \sigma_q E_q - (\delta_s + \gamma_s + \rho_s) I_s, \\ \dot{I}_i &= \tau(E_u + I_a) + \rho_s I_s - (\delta_i + \gamma_i) I_i, \\ \dot{R} &= \gamma_a I_a + \gamma_s I_s + \gamma_i I_i, \end{aligned} \tag{1}$$

where the dots on the state variables denote differentiation with respect to time. To keep track of the number of deaths, we introduce a variable  $D$  for deaths, and the equation

$$\dot{D} = \delta_s I_s + \delta_i I_i.$$

## 2.2. The behavior model

In developing the behavioral component of the model, we take into account human choice to engage in behavior that limits their contact with other humans and hence the possibility of spreading or contracting the infection. These include SQ and SD, e.g., by respecting shelter-in-place and community lockdown mandates, closure of schools and non-essential businesses, avoiding crowded environments, maintaining a safe distance from others in public, etc. With this in mind, non-quarantined susceptible individuals in the disease model (1), are players with three strategies: 1) self-quarantine or social-distance. The payoff for choosing one of the three options over the others depends on a certain cost that the individual must pay. For example, the payoff for choosing SD is that the individual will avoid becoming infected and the possibility of death from the infection, while the cost the individual must incur to achieve this is deprivation from the individual's regular activities. Here, we follow the approach of social-learning and adaptation of strategy (Bauch et al., 2005; Bhattacharyya and Bauch, 2010).

Let  $x_1(t)$  denote the fraction of non-quarantined susceptible humans who choose to SQ at time  $t$  and  $x_2(t)$  denote the fraction of non-quarantined susceptible humans who choose to SD at time  $t$ . Then  $x_3(t) = 1 - (x_1(t) + x_2(t))$  is the fraction of non-quarantined

susceptible humans who choose neither SQ nor SD. It is worth mentioning that even though humans may choose any of the first two strategies (i.e.,  $x_1$  or  $x_2$ ), they may still become infected but with a reduced probability. Hence, the perceived probability of becoming infected will be non-zero. Now, the payoff for SQ denoted by  $P_1$  is given by

$$P_1 = -[r_q + r_{sq}\psi_{sq}(m_a I_a + m_s I_s + m_i I_i)], \tag{2}$$

where  $r_q$  is the perceived cost of SQ,  $r_{sq}$  is perceived risk of infection during SQ,  $\psi_{sq}$  is a probability depicting the perceived efficacy of SQ. The payoff for SD  $P_2$ , is given by

$$P_2 = -[r_d + r_{sd}\psi_{sd}(m_a I_a + m_s I_s + m_i I_i)], \tag{3}$$

where  $r_d$  is the perceived cost of SD,  $r_{sd}$  is the perceived risk of infection during the SD, and the probability  $\psi_{sd}$  is the perceived efficacy of SD. The parameters  $m_{j,j} \in \{a, s, i\}$  reflect the respective sensitivities to acquire infection from asymptomatic infectious, symptomatic infectious, and isolated infectious individuals. The payoff for adopting none of the two strategies (SQ or SD) denoted by  $P_3$ , is given by

$$P_3 = -[r_n(m_a I_a + m_s I_s + m_i I_i) + r_\delta m_\delta(\delta_s I_s + \delta_i I_i)], \tag{4}$$

where  $r_n$  is the perceived risk of infection,  $r_\delta$  is the perceived risk of death,  $m_\delta$  is the perceived sensitivity to the prevalence of death. Generally, an individual's perception about the cost and efficacy of SQ is higher than the cost and efficacy of SD, so we assume that  $r_q \gg r_d$  and  $\psi_{sq} < \psi_{sd}$ , while the perceived risk of infection in the three strategies are opposite, i.e.,  $r_q \ll r_d \ll r_n$ . In this game theory formulation, it should be noticed that the payoff for adopting any of the three strategies depends implicitly on the strategy's history and relevant behavioral and epidemiological parameters. In particular, the current prevalence (and thus payoff) is partly determined by the history of strategies in the population. Therefore, at any given time point, individuals play not only against one another, but also against behaviorally identical individuals from previous time points. However, it may not be possible to derive a simple or closed-form expression in terms of these quantities in practice.

We also assume that individuals sample and imitate others, while deciding whether to adopt a SQ or a SD strategy against COVID-19. In particular, the decision-making involves individuals sampling others at some constant rate  $\kappa$ , and then switching to their strategy with a probability  $\nu$  that is proportional to the expected gain or payoff, if the other person's strategy provides a higher payoff. For example, the resultant payoff for switching to  $x_i$  for players (i.e., non-quarantined susceptible individuals) either in  $x_j$  or  $x_k$  is  $\Delta G_{ij} = P_i - P_j$  or  $\Delta G_{ik} = P_i - P_k$ . If both  $\Delta G_{ij}$  and  $\Delta G_{ik}$  are positive, then switching to  $x_i$  is worthwhile and the growth equation for  $x_i$  is given by

$$\dot{x}_i = x_j \kappa x_i \nu \Delta G_{ij} + x_k \kappa x_i \nu \Delta G_{ik} \tag{5}$$

$$= \mu(x_j x_i \Delta G_{ij} + x_k x_i \Delta G_{ik}), \tag{6}$$

where  $\mu = \kappa \nu$  is defined as imitation or sampling rate.

### 2.3. The coupled COVID-19 disease-human behavior model

The coupled COVID-19 disease-human behavior model is obtained by putting together Eqs. 1 and (5). This leads to the system of equations:

$$\begin{aligned} \dot{S}_u &= \xi_q S_q - (\lambda_u + \xi_u x_1) S_u, \\ \dot{S}_q &= \xi_u x_1 S_u - (\lambda_q + \xi_q) S_q, \\ \dot{E}_u &= (1 - q) \lambda_u S_u - (\alpha_u + \sigma_u + \tau) E_u, \\ \dot{E}_q &= q \lambda_u S_u + \lambda_q S_q + \alpha_u E_u - \sigma_q E_q, \\ \dot{I}_a &= f \sigma_u E_u - (\gamma_a + \tau) I_a, \\ \dot{I}_s &= (1 - f) \sigma_u E_u + \sigma_q E_q - (\delta_s + \gamma_s + \rho_s) I_s, \\ \dot{I}_i &= \tau (E_u + I_a) + \rho_s I_s - (\delta_i + \gamma_i) I_i, \\ \dot{R} &= \gamma_a I_a + \gamma_s I_s + \gamma_i I_i, \\ \dot{x}_1 &= \mu [x_1 x_2 \Delta G_{12} + x_1 (1 - x_1 - x_2) \Delta G_{13}], \\ \dot{x}_2 &= \mu [x_2 (1 - x_1 - x_2) \Delta G_{23} - x_1 x_2 \Delta G_{12}]. \end{aligned} \tag{7}$$

## 3. Results

### 3.1. Analytical results

In this section, we compute the family of disease-free equilibria and the control reproduction number of the model (7). The family of disease-free equilibria of the model system (7) obtained by setting the left hand-sides of the equations in the system to zero are given by:

$$(S_u^*, S_q^*, E_u^*, E_q^*, I_a^*, I_s^*, I_i^*, R^*, x_1^*, x_2^*) = (N(0)^* - S_q^*, -R^*, S_q^*, 0, 0, 0, 0, 0, R^*, x_1^*, x_2^*), \tag{8}$$

where  $0 < S_u^* = N(0)^* - S_q^* - R^* \leq N(0)$ ,  $0 \leq S_q^*$ ,  $R^* < N(0)$ ,  $0 < S_u^* + S_q^* + R^* \leq N(0)$ , and

$$\begin{aligned} S_q^* &= \frac{\xi_u}{\xi_q} x_1^* S_u^*, \\ (x_1^*, x_2^*) &\in \left\{ (0, 0), (1, 0), (0, 1), \left( \frac{\Delta G_{23}^*}{\Delta G_{12}^* + \Delta G_{13}^* + \Delta G_{23}^*}, \frac{\Delta G_{13}^*}{\Delta G_{12}^* + \Delta G_{13}^* + \Delta G_{23}^*} \right) \right\} \\ &= \left\{ (0, 0), (1, 0), (0, 1), \left( \frac{r_d}{2r_q}, \frac{1}{2} \right) \right\} \end{aligned}$$

The control reproduction number of the model tracks the average number of secondary infections produced by one infectious human in a population taking into account some control measures over the time frame within which the infectious individual can spread the disease. We apply the next generation matrix approach Diekmann et al., 1990; van den Driessche and Watmough, 2002 to compute the reproduction number of the model system (7). This involves constructing a matrix of new infections  $\mathcal{F}$ , a matrix of transitions  $\mathcal{V}$ , and determining the spectral radius of the matrix product  $\mathcal{F} \mathcal{V}^{-1}$ . Following this approach, the matrices  $\mathcal{F}$ ,  $\mathcal{V}$ , and  $\mathcal{V}^{-1}$  are

$$\mathcal{F} = \begin{pmatrix} 0 & 0 & \frac{(1-q)(1-\epsilon x_2^*) \beta_u S_u^*}{S_u^* + (1-\omega_q) S_q^* + R^*} & \frac{(1-q)(1-\epsilon x_2^*) \beta_s S_u^*}{S_u^* + (1-\omega_q) S_q^* + R^*} & \frac{(1-q)(1-\epsilon x_2^*) \eta_i \beta_s S_u^*}{S_u^* + (1-\omega_q) S_q^* + R^*} \\ 0 & 0 & \frac{\beta_u (q(1-\epsilon x_2^*) S_u^* + \phi_q S_q^*)}{S_u^* + (1-\omega_q) S_q^* + R^*} & \frac{\beta_s (q(1-\epsilon x_2^*) S_u^* + \phi_q S_q^*)}{S_u^* + (1-\omega_q) S_q^* + R^*} & \frac{\eta_i \beta_s (q(1-\epsilon x_2^*) S_u^* + \phi_q S_q^*)}{S_u^* + (1-\omega_q) S_q^* + R^*} \\ 0 & 0 & 0 & 0 & 0 \\ 0 & 0 & 0 & 0 & 0 \\ 0 & 0 & 0 & 0 & 0 \end{pmatrix},$$

$$\mathcal{V} = \begin{pmatrix} A_u & 0 & 0 & 0 & 0 \\ -\alpha_u & \sigma_q & 0 & 0 & 0 \\ -f\sigma_u & 0 & A_a & 0 & 0 \\ -(1-f)\sigma_u & -\sigma_q & 0 & A_s & 0 \\ -\tau & 0 & -\tau & -\rho_s & A_i \end{pmatrix}, \text{ and}$$

$$\mathcal{V}^{-1} = \begin{pmatrix} \frac{1}{A_u} & 0 & 0 & 0 & 0 \\ \frac{\alpha_u}{\sigma_q A_u} & \frac{1}{\sigma_q} & 0 & 0 & 0 \\ \frac{f\sigma_u}{A_a A_u} & 0 & \frac{1}{A_a} & 0 & 0 \\ \frac{(1-f)\sigma_u + \alpha_u}{A_s A_u} & \frac{1}{A_s} & 0 & \frac{1}{A_s} & 0 \\ \frac{(1-f)\rho_s \sigma_u A_a + f\tau \sigma_u A_s + \tau A_a A_s + \rho_s \alpha_u A_a}{A_a A_i A_s A_u} & \frac{\rho_s}{A_i A_s} & \frac{\tau}{A_a A_i} & \frac{\rho_s}{A_i A_s} & \frac{1}{A_i} \end{pmatrix},$$

where

$$A_u = \alpha_u + \sigma_u + \tau, A_a = \gamma_a + \tau, A_s = \delta_s + \gamma_s + \rho_s, A_i = \delta_i + \gamma_i. \quad (9)$$

The reproduction number of system (7),  $\mathcal{R}_c$ , i.e., the spectral radius of the matrix product  $\mathcal{F}\mathcal{V}^{-1}$  is:

$$\mathcal{R}_c = \mathcal{R}_a + \mathcal{R}_s + \mathcal{R}_i, \quad (10)$$

where

$$\mathcal{R}_a = \frac{(1-q)f(1-\epsilon x_2^*)\beta_a \sigma_u S_u^*}{[S_u^* + (1-\omega_q)S_q^* + R^*]A_a A_u}, \quad \mathcal{R}_s = \frac{\beta_s \{(1-\epsilon x_2^*)\} \{(1-q)[(1-f)\sigma_u + \alpha_u] + qA_u\} S_u^* + \phi_q A_u S_q^*}{[S_u^* + (1-\omega_q)S_q^* + R^*]A_s A_u}$$

$$\mathcal{R}_i = \frac{\eta_i \beta_i \{(1-\epsilon x_2^*)\} \{(1-q)[(1-f)\rho_s \sigma_u A_a + \tau A_s (f\sigma_u + A_a) + \rho_s \alpha_u A_a] + q\rho_s A_a A_u\} S_u^* + \phi_q \rho_s A_a A_u S_q^*}{[S_u^* + (1-\omega_q)S_q^* + R^*]A_a A_i A_s A_u}.$$

As in Ngonghala et al. (2020a,b), the reproduction number  $\mathcal{R}_c$ , is the sum of three terms associated with disease transmission by asymptomatic infectious humans  $\mathcal{R}_a$ , disease transmission by symptomatic infectious humans  $\mathcal{R}_s$ , and isolated infectious humans  $\mathcal{R}_i$ . Additionally, the reproduction number is a function of the equilibrium values of  $x_1^*$  and  $x_2^*$ , and when  $S_q^* = R^* = 0$ ,  $\mathcal{R}_a$ ,  $\mathcal{R}_s$ , and  $\mathcal{R}_i$  reduce to:

$$\mathcal{R}_a = \frac{(1-q)f(1-\epsilon x_2^*)\beta_a \sigma_u}{A_a A_u}, \quad \mathcal{R}_s = \frac{(1-\epsilon x_2^*)\beta_s \{(1-q)[(1-f)\sigma_u + \alpha_u] + qA_u\}}{A_s A_u},$$

$$\mathcal{R}_i = \frac{(1-\epsilon x_2^*)\eta_i \beta_i \{(1-q)[(1-f)\rho_s \sigma_u A_a + \tau A_s (f\sigma_u + A_a) + \rho_s \alpha_u A_a] + q\rho_s A_a A_u\}}{A_a A_i A_s A_u}.$$

Using the parameter values in Table S1 in SI, the value of the basic reproduction number is  $R_0 = 2.7$ . It should be mentioned that this is computed for the scenario in which  $(x_1^*, x_2^*) = (0, 0)$ . Fig. 2 shows a heat map of the reproduction number  $R_c$ , as a function of the equilibrium proportion of non-quarantined susceptible humans who choose SD and (a) the efficacy of social-distancing  $\epsilon$ , and (b)-(c) the detection or isolation rate of exposed and asymptomatic infectious individuals,  $\tau$ . Increases in the number of non-quarantined susceptible humans who choose SD and the efficacy of SD will lead to a decrease in the control reproduction number, and hence dis-

ease burden (Fig. 2(a)). However, for an appreciable decrease in disease burden and possible elimination, both  $x_2^*$  and  $\epsilon$  must be high. For example, if 84% of the population choose SD, then an efficacy of at least 83% is required to contain the pandemic. Unfortunately, it is difficult to achieve this high level of SD and efficacy in any community. Although combining SD with other measures is a better approach to fight COVID-19 (see, for example, Ngonghala et al., 2020), this study shows that the efficacy of SD must be high. Specifically, containing the pandemic will be impossible for moderately efficacious SD (e.g.,  $\epsilon = 0.5$ ), even if high SD is combined with high case detection (Fig. 2(b)). However, if the efficacy is increased to 80% and the detection rate is  $\tau = 0.57$ , then at least 75% of the population is required to engage in SD in order to reduce the reproduction number below unity (Fig. 2(b)).

### 3.2. Numerical simulation results

In this section, we simulate the model system (7) to illustrate the impact of human response to social-isolation (i.e., SQ and SD) on the evolution of the COVID-19 outbreak. These simulations are carried out using parameter values that are drawn either from the literature, estimated from available information or through educated guesses (Table 1 in the SI). Except otherwise stated, the initial conditions used for the simulations are:  $S_u(0) = 0.99997$ ,  $S_q(0) = 0$ ,  $E_u(0) = 0$ ,  $E_q(0) = 0$ ,  $I_a(0) = 0.00001$ ,  $I_s(0) = 0.00001$ ,  $I_i(0) = 0.00001$ ,  $R(0) = 0$ ,  $D_0 = 0$ ,  $x_1 = 0.04$  and  $x_2 = 0.8$ . The total population is assumed to be 100,000 for qualitative analysis of the model. Also, we used COVID-19 and lockdown data from India to estimate some of the key model parameters and to perform a scenario analysis to assess the impact of relaxation of lockdown measures and extension or implementation of lockdown measures at different time periods on the COVID-19 pandemic in India.

#### 3.2.1. Impact of self-quarantine (SQ) versus social-distancing (SD)

Different countries embarked on different types and stringency levels of social-isolation measures to reduce the burden of the COVID-19 pandemic. The type and stringency level of social-isolation implemented by a country was determined primarily by the availability of public health personnel, infrastructure, personal protection equipment, and the state of the economy of the country. In particular, public health authorities from many High Income Countries (HIC) promoted SQ of suspected cases and “shelter-in-place” or country-wide lockdown, whereas many Low and Middle Income Countries (LMIC) preferred other less stringent forms of SD (Gelfand et al., 2020; Germani et al., 2020; Walker et al., 2020; Travaglino and Moon, 2020). Each of these strategies is associated with a cost to individuals and whole communities. For example,

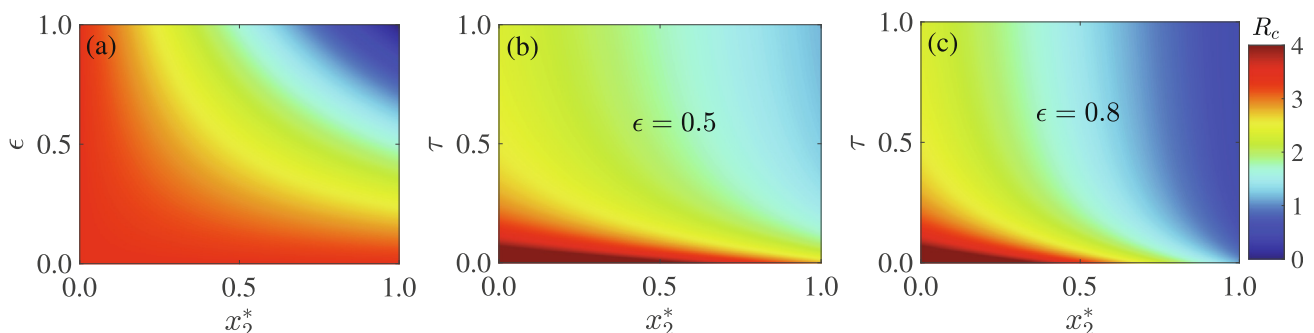
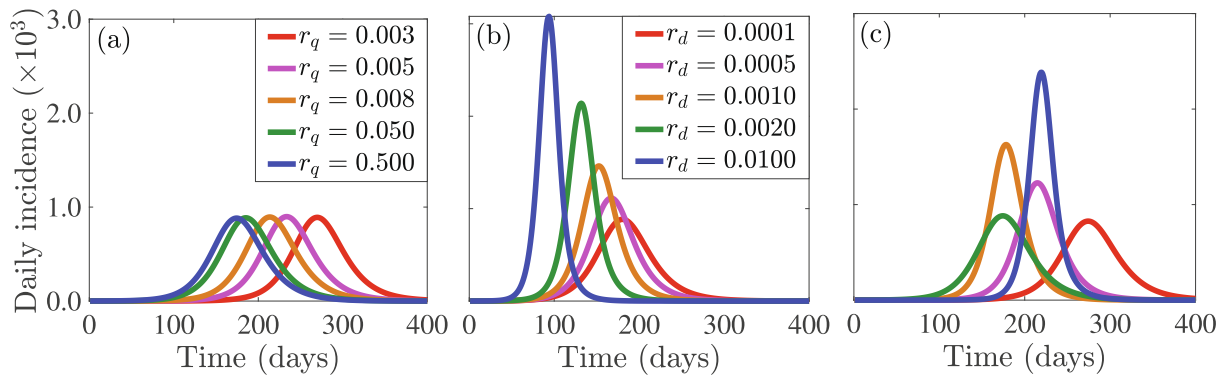


Fig. 2. Heat map of the reproduction number  $R_c$ , as a function of the equilibrium fraction of humans who choose SD ( $x_2^*$ ), and (a) the efficacy of SD ( $\epsilon$ ), (b) case detection rate ( $\tau$ ) when  $\epsilon = 0.5$ , and (c)  $\tau$  when  $\epsilon = 0.8$ .



**Fig. 3.** Time series plots of COVID-19 incidence from simulations of the model system (7) for different values of the perceived cost of (a) SQ ( $r_q$ ) for  $r_d = 0.0001$ , (b) SD ( $r_d$ ) for  $r_q = 0.1$ , and (c) SQ and SD for  $r_q = 0.003, r_d = 0.0001$  (red curve),  $r_q = 0.005, r_d = 0.0005$  (magenta curve),  $r_q = 0.008, r_d = 0.001$  (gold curve),  $r_q = 0.5, r_d = 0.0001$  (green curve),  $r_q = 0.003, r_d = 0.01$  (blue curve). Observe that the perceived cost of SQ has relatively less impact on daily incidence peak compared to the perceived cost of SD. The other initial conditions and parameter values used for the simulations are presented in Section 3.2 and Table S1 in SI.

lockdown comes at a cost that includes loss of jobs and earnings. This can lead to be devastating, especially for low-income earners and it can also impact the mental health and well-being of victims negatively (Brooks et al., 2020). Self-quarantine is also associated with a significant cost, e.g., isolation from contacts and routine activities, which can also have a negative impact on an individual's mental health. This perceived cost for SQ adds up fast in LMICs owing to additional quarantine-induced issues such as anxiety and various forms of insecurity (European Centre for Disease Prevention and Control, 2020). Hence, the choice of SD or SQ depends on the perceived cost of the strategy. To assess the impact of this perceived cost on the burden of COVID-19 (measured in terms of the number of new daily cases, i.e., the daily incidence), we simulate the model (7) for different values of the perceived cost of SQ ( $r_q$ ) and SD ( $r_d$ ) (Fig. 3). The simulation results show that small changes in the perceived cost of SD have a big impact on the incidence (i.e., the new daily cases) of COVID-19 compared to small changes in the perceived cost of SQ. In particular, decreasing the perceived cost of SD from 0.01 (blue curve in Fig. 3(b)) to 0.0001 (red curve in Fig. 3(b)) will result in a drastic 71% decrease in disease incidence when the pandemic peaks and an 86-day increase in the time at which the pandemic peaks. On the other hand, decreasing the perceived cost of SQ does not have any significant impact on the size of the pandemic peak. However, decreasing the perceived cost of SQ leads to a delay in the time at which

the pandemic peaks (without decreasing the cumulative incidence). For example, decreasing the perceived cost of SQ from 0.5 (blue curve in Fig. 3(a)) to 0.003 (red curve in Fig. 3(a)) will result in a 97-day (i.e., 56%) increase in the time at which the pandemic peaks. This shows that SD is more effective in mitigating the COVID-19 pandemic, especially if the perceived cost of SD is low. In particular, if the perceived costs of both SQ and SD are high, then a high number of daily cases will be recorded when the pandemic peaks and the peak will occur earlier (blue curve in Fig. 3(c)) compared to the case when the perceived costs of both SQ and SD are low (red curve in Fig. 3(c)).

### 3.2.2. Influence of initial players

The population of initial players playing each strategy in the beginning of the outbreak always influences the game and hence dynamics of SD and disease outbreak. To investigate this, we use different initial values of  $x_1$  for SQ and  $x_2$  for SD, where different initial values for  $x_1$  (respectively,  $x_2$ ) reflect different fractions of members of the community who have adopted SQ (respectively, SD). The results depicted in Fig. 4 indicate that variation in the initial proportion of individuals adopting SQ are less impactful to the incidence pattern, e.g., the outbreak size, especially for low values of  $x_1(0)$  (Fig. 4(a)). In particular, if the initial proportion of individuals who adopt SQ increases from 0.02 to 0.60, a 15% decrease in the daily incidence is recorded on the day the pandemic peaks

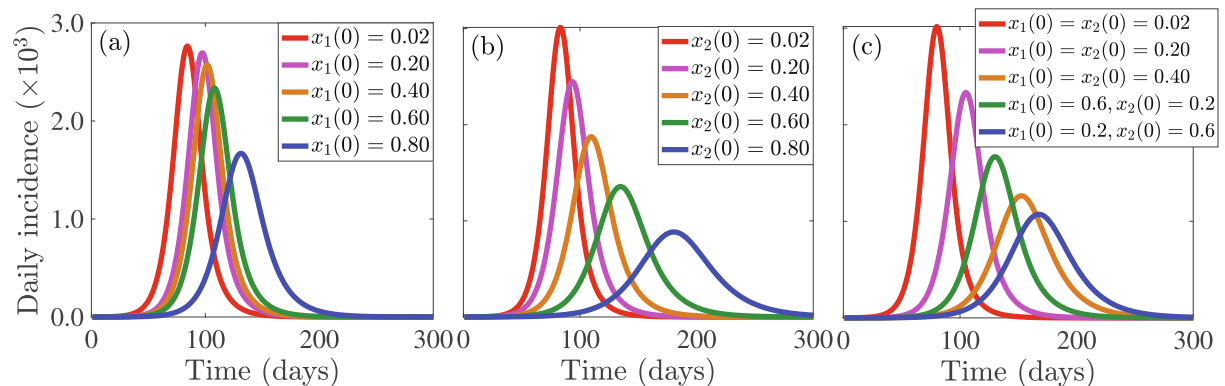


**Fig. 4.** Simulation results of the model (7) showing the daily disease incidence as a function of time for two disease control strategies: (a) self-quarantine (SQ) quantified in terms of the initial proportion of the population who choose SQ ( $x_1(0)$ ) with  $r_q = 0.1, r_d = 0.0001$ , and  $x_2(0) = 0.1$ , (b) social-distancing (SD) quantified in terms of the initial proportion of the population who choose SD ( $x_2(0)$ ) with  $r_q = 0.1, r_d = 0.0001$ , and  $x_1(0) = 0.04$ , and (c) SQ and SD measured in terms of ( $x_1(0)$ ) and ( $x_2(0)$ ) with  $r_q = 0.1, r_d = 0.0001$ . Different fractions of initial populations enable individuals to imitate others more and choose their strategies. The other initial conditions and parameter values used for the simulations are presented in Section 3.2 and Table S1 in SI.

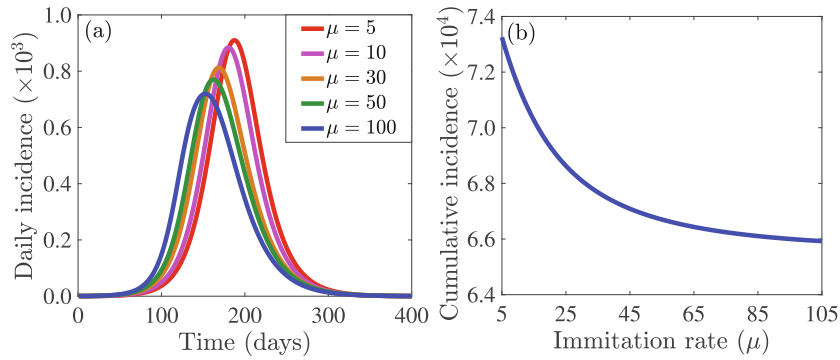


**Fig. 5.** Simulations of the model (7) to assess the effects of the sampling or imitation rate ( $\mu$ ) of others choices of social-isolation on the: (a) daily incidence of COVID-19, and (b) cumulative incidence of COVID-19. The initial values of  $x_1$  and  $x_2$  are  $x_1(0) = 0.2$  and  $x_2(0) = 0.5$  and the other initial conditions are presented in Section 3.2. The other parameter values used for the simulations are presented in Table S1 in SI.

(green curve in Fig. 4(a)). A further increase by 0.20, i.e., an increase from 0.02 to 0.80 will lead to a 40% reduction in the daily incidence on the day the pandemic peaks (blue curve in Fig. 4(a)). On the contrary, variation in the initial proportion of individuals who adopt SD has a more significant impact on disease compared to SQ (Fig. 4(b)). Specifically, the more the initial proportion of the population that adopts SD (from the onset of the outbreak), the higher the possibility of more people adopting the SD strategy. This will lead to a lower disease burden (i.e., lower cumulative incidence, as well as a lower and delayed pandemic peak size). For example, if the initial proportion of individuals who adopt SD increases from 0.02 to 0.60, the number of new daily COVID-19 cases decreases by approximately 55% on the day the pandemic peaks (green curve in Fig. 4(a)). This represents a 40% additional decrease in daily incidence on the day the pandemic peaks compared to the same 0.02 to 0.60 increase in the initial proportion of individuals who adopt SQ (green curves in Fig. 4(a) and (b)). Furthermore, if the initial proportion of individuals who adopt SD increases from 0.02 to 0.80, the number of new daily COVID-19 cases decreases by approximately 71% on the day the pandemic peaks (blue curve in Fig. 4(b)). This represents a 31% additional decrease in daily incidence on the day the pandemic peaks compared to the same 0.02 to 0.60 increase in the initial proportion of individuals who adopt SQ (blue curves in Fig. 4(a) and (b)). On the other hand, if the initial proportion of individuals who adopt SQ increases from 0.02 to 0.60 and the initial proportion of individuals who adopt SD is maintained at 0.02, then approximately 45% of the number of new cases on the day the pandemic peaks will be

averted (green curve in Fig. 4(c)), while if the initial proportion of individuals who adopt SD increases from 0.02 to 0.60 and the initial proportion of individuals who adopt SQ is maintained at 0.02, then approximately 64% of the number of new cases on the day the pandemic peaks will be averted (blue curve in Fig. 4(c)). This, shows that SD is more important in reducing the number of COVID-19 cases and in delaying and/or slowing down the transmission of COVID-19. Heatmaps depicting the impact of SD and SQ on the daily incidence peak and symptomatic cases is presented in Fig. S1 in SI. The public health implication of this result is that public health authorities should promote SD through various media outlets to enable individuals to sample and possibly adopt SD.

### 3.2.3. Impact of sampling or imitation rate

Media coverage and social networking play an important role in individual decision-making during SD. We carried out simulations to assess the impact of the rate at which people sample the behaviors/decisions of others on the burden of the outbreak measured in terms of the daily and cumulative incidence (Fig. 5). The results indicate that increasing the sampling rate does not have much impact on the daily outbreak pattern, but it leads to a decrease in the cumulative incidence. This is reasonable since sampling will increase the number of people who switch to both strategies (i.e., SQ and SD) proportionately at higher rates, which in turn, leads to faster decay of infection in the community. This signifies the fact that more sampling can bring about a reduction in the burden of COVID-19. The public health implication of this result is that

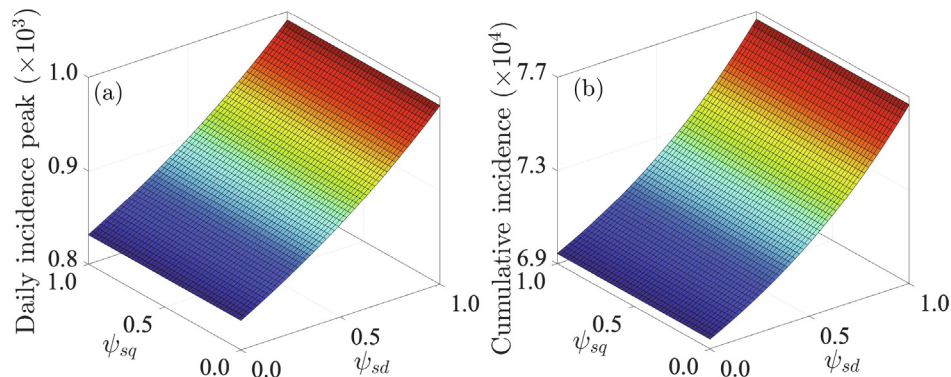


**Fig. 6.** Surface plot of the (a) peak incidence and (b) cumulative incidence as functions of the perceived efficacy of SD ( $\psi_{sd}$ ) and the perceived efficacy of SQ ( $\psi_{sq}$ ). It should be noted that there is a nonlinear relationship between the peak incidence and the parameters  $\psi_{sd}$  and  $\psi_{sq}$ , as well as between the cumulative incidence and the parameters  $\psi_{sd}$  and  $\psi_{sq}$ . For example, the cumulative incidence increases as the perceived efficacy of SD  $\psi_{sd}$ , decreases (or as the probability of infection increases), while the efficacy of SQ has almost no impact on the cumulative incidence. Initial conditions are presented in Section 3.2 and the other parameters used for the simulations are presented in Table S1 in SI.

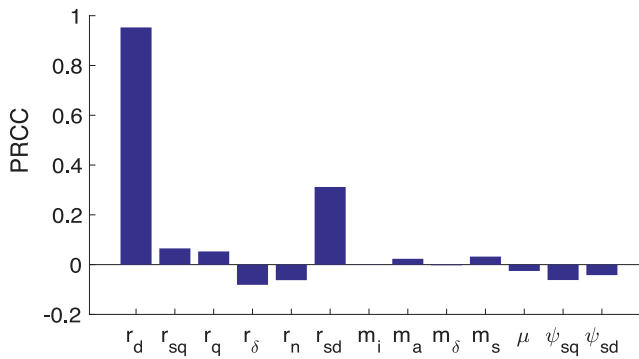


**Fig. 7.** A tornado plot with PRCCs depicting the significant dependence of daily incidence on behavioral parameters. Using Latin Hypercube Sampling (LHS) McKay et al., 2000, 1000 samples were drawn from uniform distribution of the parameter ranges without replacement:  $r_q = [0.004, 0.3]$ ,  $r_{sq} = [0.03, 0.5]$ ,  $r_{sd} = [0.08, 0.3]$ ,  $r_n = [0.03, 0.09]$ ,  $r_d = [0.001, 0.1]$ ,  $m_i = [0.4, 0.82]$ ,  $m_a = [0.72, 0.75]$ ,  $m_s = [0.7, 0.8]$ ,  $m_\delta = [0.007, 0.01]$ ,  $\mu = [9, 50]$ ,  $\psi_{sq} = [0.08, 0.5]$  and  $\psi_{sd} = [0.0001, 0.09]$ . The initial conditions are  $S_u(0) = 0.76$ ,  $S_q(0) = 0$ ,  $E_u(0) = 0$ ,  $E_q(0) = 0$ ,  $I_a(0) = 0.00001$ ,  $I_s(0) = 0.00001$ ,  $I_i(0) = 0.00001$ ,  $R(0) = 0$ ,  $D_0 = 0$ ,  $x_1 = 0.04$  and  $x_2 = 0.2$ . The span of the time series considered in this PRCC analysis is [1,360].

widespread media coverage on SQ and SD mitigation strategies can educate and influence more people to adopt the right strategy.

### 3.2.4. Efficacy of social-isolation

Simulations of the model (7) were also carried out to investigate the influence of the perceived efficacy of SD ( $\psi_{sd}$ ) and SQ ( $\psi_{sq}$ ) on the incidence peak size (Fig. 6(a)) and cumulative incidence of COVID-19 (Fig. 6(b)). Higher values of  $\psi_{sd}$  and  $\psi_{sq}$  correspond to lower efficacy of the respective strategies (SD and SQ) and hence, a higher disease burden. Our simulations show that both the incidence peak size and cumulative incidence of COVID-19 increase with increasing perceived efficacy of SD values, but does not vary significantly with changes in the perceived efficacy of SQ. In particular, high values of  $\psi_{sd}$  can produce a huge and intense outbreak. This suggests that it is more feasible to adopt SD as a strategy to combat COVID-19 compared to SQ. Furthermore, combining both SD and SQ strategies is more effective in combating the pandemic than using only a single strategy.

### 3.2.5. Sensitivity of behavior-related parameters

To assess the impact of uncertainty and variability in behavior-related parameters to model outputs such as the daily incidence, and to identify parameters that impact model outputs significantly,

we use the Latin Hypercube Sampling and Partial Rank Correlation Coefficients (PRCCs) techniques (Marino et al., 2008; Blower and Dowlatabadi, 1994) to carry out a global uncertainty and sensitivity analysis. The results depicted in Fig. 7 show that all risk-related parameters ( $r_q$ ,  $r_d$ ,  $r_{sq}$ , and  $r_{sd}$ ) are positively correlated with disease incidence as reflected in the time series simulations. The results also show that the perceived cost of SD,  $r_d$ , has the greatest impact on disease incidence compared to the other risk-related parameters. Also,  $\psi_{sd}$  has relatively more significant impact on disease incidence than  $\psi_{sq}$ , which is in agreement with the results in Fig. 6. Furthermore, the results show that the sampling rate,  $\mu$ , does not have a significant impact on the incidence, which is in conformity with the results presented in Fig. 5. In summary, the global uncertainty and sensitivity analysis results suggest that the perceived risks of social-isolation have variable, but significant impact on the dynamics of COVID-19 incidence.

### 3.2.6. Mandatory vs. Voluntary self-quarantine (SQ) and social-distancing (SD)

Both SQ and SD have been useful in reducing the burden of the COVID-19 pandemic in many countries. Whether these measures are implemented voluntarily by individuals or imposed by the government is important for the success of control program that relies on these measures. Here, we simulate the model (7) to assess the impact of implementing both measures through a mandatory and voluntary approach on the transmission dynamics of the disease. For this purpose, we reduce our 3-strategy model framework to a 2-strategy framework by restricting one of the strategy-variable ( $x_i, i \in \{1, 2\}$ ) to be constant implying a mandatory implementation of that specific social-isolation mechanism. The results of our analysis are presented in Fig. 8, with dashed blue curves depicting the pattern of disease outbreak when both strategies are voluntary (i.e., when individuals choose to adopt both SQ and SD voluntarily), and solid red curves depicting epidemic patterns when both strategies are mandatory (i.e., when both SQ and SD are imposed by the government). As expected, the size of the pandemic peak is very high when individuals are allowed to decide whether to implement both strategies or not compared to when the strategies are imposed by the government. This is because whether an individual adopts a strategy or not depends on the probability of infection and the severity of the spread, which is generally lower at the beginning of the outbreak. Thus, fewer individuals adopt both strategies voluntarily and consequently this leads to increased transmission or an increase in the size of the outbreak. In particular, there is a drastic (approximately 85%) reduction in the size of the pandemic peak when SD and SQ is

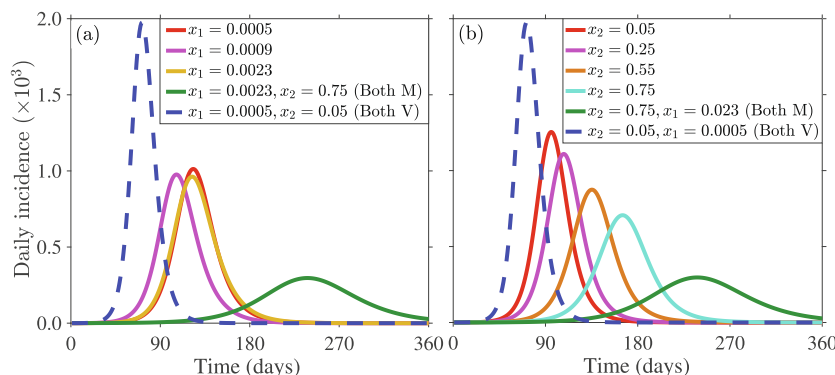


**Fig. 8.** Time series plots of daily incidence from simulations of the model (7) for different values of: (a) mandatory self-quarantine (SQ) levels with voluntary social-distancing (SD), and (b) mandatory SD strictness levels with voluntary SQ. The dashed blue and the solid red curves in both plots depict the respective impacts a combined voluntary SQ and SD measure and a mandatory SQ and SD measure on disease incidence. The initial conditions and parameter values used for the simulations are presented in Section 3.2 and Table S1 in SI.

mandatory (green curves in Fig. 8(a) and (b)) compared to when both strategies are voluntary (green dashed blue curves in Fig. 8(a) and (b)). On the other hand if SQ is mandatory, while SD is voluntary, then increasing the stringency of SQ does not impact the size of the pandemic peak significantly. However, the time at which the peak occurs is prolonged. On the contrary, if SQ is voluntary while SD is mandatory, then increasing the coverage or stringency of SD reduces the size of the pandemic peak significantly. In particular, if SD is mandatory, and the coverage or stringency of SD is increased from 0.05 (red curve in Fig. 8(b)) to 0.75 (cyan curve in Fig. 8(b)), the size of the pandemic peak is reduced by approximately 40%, while the time at which the peak occurs increases by approximately 60%. This suggests that as a single mandatory measure, mandatory SD is more effective than mandatory SQ in minimizing the burden of the COVID-19 pandemic.

Additional simulations were carried out to assess the impact of alternating implementation of the mandatory and voluntary social-isolation measures on the burden of the pandemic. This entails imposing a mandatory strategy for some time period, switching the same strategy to voluntary for the next time period, and then switching back to mandatory, etc. We implement each of the strategies (SQ and SD) as *Voluntary-Mandatory-Voluntary-Mandatory*, within certain fixed periods of time by keeping the end point of the chosen strategy's variable ( $x_i$ ) constant for mandatory implementation or the initial population for voluntary implementation. Fig. 9 shows the effect of such an implementation separately for SD (Fig. 9(a) and (c)) and SQ (Fig. 9(b) and (d)). We also show the counterfactual by comparing the relative impacts of such implementing such an alternating *Voluntary-Mandatory-Voluntary-Mandatory* strategy. Simulations of the model (7) with a *Mandatory-Voluntary* combination approach illustrates that reducing cumulative incidence is not always helpful. For example, Fig. 9(a) and (b) shows that implementing this alternating combination

approach may reduce the incidence peak size, but at the same time, the duration of the outbreak may increase. This might trigger an increase in the cumulative incidence. Fig. 9(c) and (d) shows that SQ is instrumental in reducing the cumulative incidence by this alternating combination approach (Fig. 9(c)), while SD implementation results in an increase in cumulative incidence (Fig. 9(d)). This is due to the fact that the efficacy of SQ is higher than that of SD, while the probability of infection is lower.

We also simulate the model (7) to explore the effects of timing of the alternative implementation of the *Mandatory-Voluntary* approach to social-isolation under five different scenarios describing different implementation time points. Our results show that there are significant qualitative and quantitative differences in the pandemic outbreak size and the time that elapses before the pandemic peaks for each of the two social-isolation mechanisms (Fig. 10). In particular, early implementation of mandatory SD is important in reducing disease transmission (Fig. 10(a)). This is not exactly the same case with SQ, where the peak size is lower, if mandatory SQ is implemented later in the course of the outbreak (Fig. 10(b)). This is because the efficacy of SQ is higher than that of SD.

#### 4. Data, implementation and parameter estimation

In this section, we use different COVID-19 related data sets from India obtained from various sources including Roser et al. (2020) to estimate key behavioral and COVID-19 transmission related parameters of the model (7). These parameters include the community transmission rate  $\beta_i, i \in \{a, s\}$ , risk-related parameters  $r_q, r_d$ , and  $r_\delta$ , behavioral parameters  $\mu, \psi_{sq}$ , and  $\psi_{sd}$ , and reporting probability. Daily incidence data of COVID-19 for India for the period from January 22 to July 20, 2020 (Fig. S2 in SI)

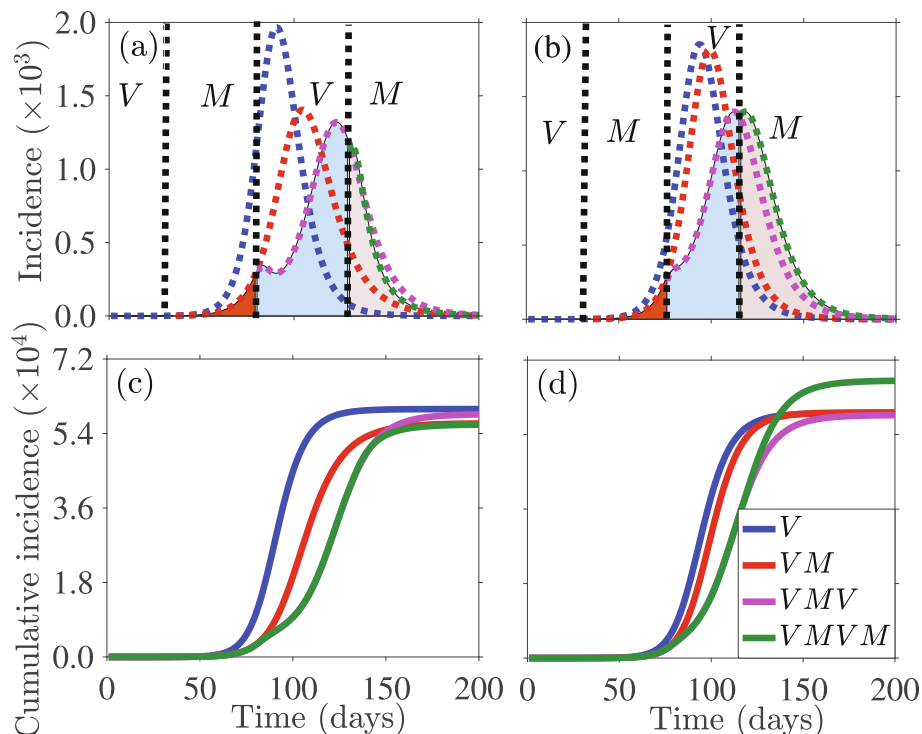


**Fig. 9.** Simulations of the model (7) depicting the daily and cumulative disease incidence under alternating combinations of *Mandatory-Voluntary* approaches of social-isolation: SD ((a) and (c)), and SQ((b) and (d)). The time points for strategy-switching implementation in each case is day 30, 80, and 130. The counterfactual is represented by dotted lines, and are used to compare the effect in absence of further implementation. The initial conditions and parameter values used for the simulations are presented in Section 3.2 and Table S1 in SI.

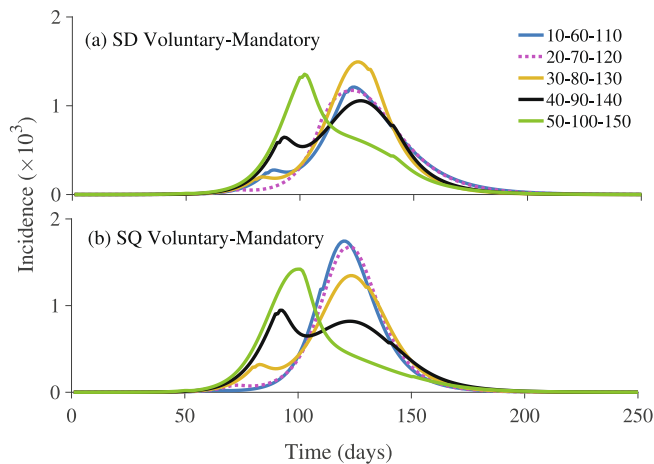


**Fig. 10.** Simulations of the model (7) depicting the outbreak pattern of the COVID-19 pandemic under combinations of *Mandatory-Voluntary* approaches for (a) social-distancing (SD), and (b) self-quarantine (SQ) at different time points (presented in the Fig. legends). The initial conditions and parameter values used for the simulations are presented in Section 3.2 and Table S1 in SI.

was drawn from various sources including the World Health Organization (WHO) website (World Health Organization, 2020), the John Hopkins COVID-19 dashboard (Dong et al., 2020; World Health Organization, 2020), and Worldometer (2020). COVID-19 testing numbers in India have been extremely variable throughout the COVID-19 period. This variability has a big influence on the case detection rate ( $\tau$ ) in the model (7). Hence, we include testing related data obtained from Roser et al. (2020) in the parameter estimation (Fig. S3 in SI). During the COVID-19 pandemic, many countries including India implemented social-isolation through a *voluntary-mandatory* approach, i.e., a voluntary approach was first adopted for some period (specifically around the onset of the pandemic) before switching to a mandatory approach for a while, and then returning to the voluntary approach. For example, strict countrywide lockdown was implemented in India on March 23, 2020 and then either continued or relaxed under different circumstances such as workplace, transport, schools, markets, etc. Implementation of social-isolation and strictness in measure during COVID related lockdown in India is presented in Fig. S6 in SI (data obtained from Roser et al., 2020). The stringency of the lockdown measures implemented by the Indian government changed over time in response to the burden of the pandemic (Fig. S4 in SI). At the time this study was carried out, there was no data or direct information at the individual level on how individual perception of the risk of infection changes and how individuals reacted to the lockdown and social-isolation measures implemented during the COVID-19 outbreak. We used data on the proportion of visitors in recreation centers, parks, grocery stores, workplaces, etc., as proxies to such individual level perceptions (Fig. S5 in SI). Also, we used detailed information including dates and strictness level of lockdown to train our model for the specific case of India. We used all these data to train our model in our parameter estimation. The detailed methodology and parameter estimation process is presented in the SI. As depicted in the model fit Fig. 11, the model (7) captures the pattern of exponential growth shown in the case data nicely. The estimated parameter values are presented in Table S2 in SI, while the other model parameters which are not estimated here, were drawn from the literature (Ngonghala et al., 2020). For this parameter regime, the value of the basic reproduction is approximately 2.7.

## 5. Scenario analysis using the estimated model parameter values

We perform different *what-if* scenario analyses with the parameter values estimated using COVID-19 incidence and control data from India. Our analyses are based on three different scenarios, each of which evaluates the impact of strict implementation of mandatory lockdown relative to individual voluntary implementation of social-isolation to reduce the community transmission of COVID-19: (I) relaxation of strict lockdown, (II) extension of the strict lockdown period, and (III) initiation of lockdown at different dates. Our analysis show that relaxing the strict mandatory SQ or stay-at-home measure from March 23 to May 6, 2020 would have triggered an increase in the daily incidence of COVID-19 in India by approximately 68.8% (Fig. 12 (a)), whereas relaxing only the SD measure would have increased the daily disease incidence by only 13%. Relaxing both the mandatory SQ and lockdown will result in a catastrophic explosion in the daily number of cases. This indicates that strict mandatory social-isolation was very useful in curbing the transmission of COVID-19 in India.

Additional simulations were carried out to assess the effects of extending the strict mandatory countrywide lockdown in India beyond May 6, 2020 (Fig. 12 (b)). Here we extend both the SQ and SD. Extending the strict lockdown for another 15, 30, 45, and 60 days would have reduced the daily incidence peak of COVID-19 in India by approximately 35%, 67%, 74%, and 83%, respectively, (Fig. 12(b)). On the other hand, the precise time at which lockdown is implemented in the course of the pandemic can have a significant impact on the burden of the pandemic. Hence, we also carried out simulations to investigate the effects of implementation of lockdown at different time points on the daily incidence of COVID-19 in India (Fig. 12(c)). The result of the simulation (c) indicates that implementation of the lockdown measure on March 1, 2020 and maintaining strict lockdown for one and half months does not play a role in reducing the daily incidence of the disease, rather it increases the daily incidence approximately 36%. Similarly, implementation of a lockdown mandate on March 15, 2020 would have resulted in a 7% increase in the number of new daily cases. In contrast, imposing strict lockdown measures on March 30, 2020 (or April 10, 2020) would have triggered a 10% (or 26%) decrease in the number of new daily COVID-19 cases in India. This scenario analysis indicates that mandatory strict lockdown is useful in reducing COVID-19 transmission in India. However, an optimal design of lockdown measure that takes into account the type of lockdown, initiation date of the lockdown,

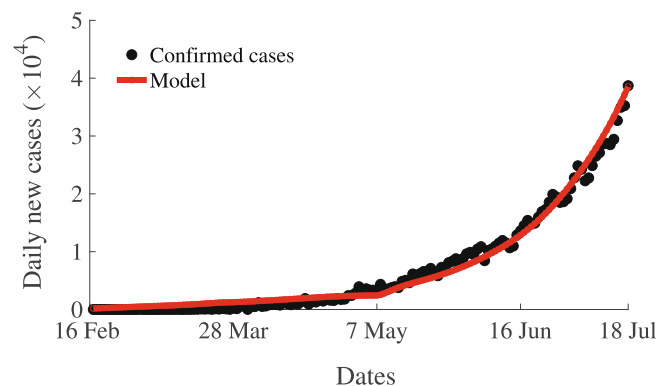


**Fig. 11.** Model fit to the confirmed new daily COVID-19 cases in India for the period from February 16 to July 20, 2020. Filled black circles represent the actual confirmed daily COVID-19 cases, while the solid red curve represents the prediction of the new daily cases from the model (7). The other parameters that are not estimated here are presented in Table S1 in SI.

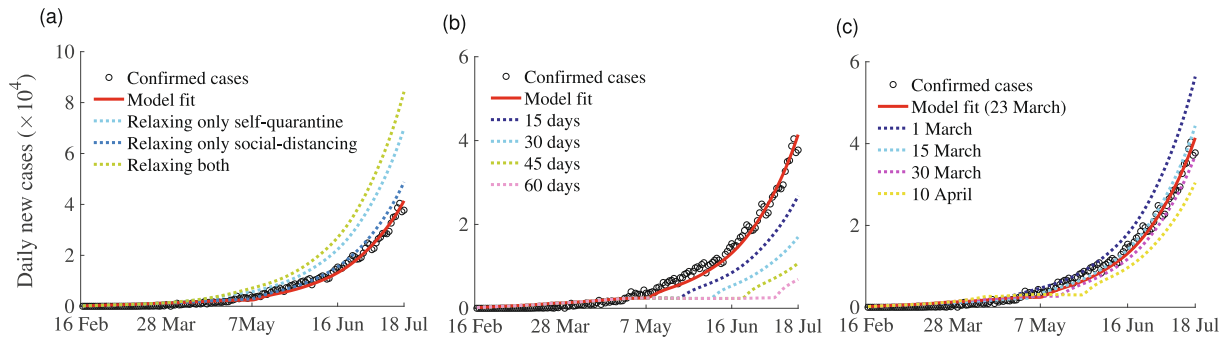


**Fig. 12.** Simulations of the model (7) to assess three COVID-19 control-related scenarios. (a) Scenario I: Mandatory strict lockdown is relaxed (i.e., it is voluntary) from March 23 to April 19, 2020. SQ and SD are relaxed separately and together. (b) Scenario II: Mandatory strict lockdown is extended from May 6 by several days, e.g., 15, 30, 45, and 60 days. (c) Scenario III: Mandatory strict lockdown is implemented on different dates, e.g., March 1, 15, 30, and April 10, 2020. For more explanation, see the text.

and the duration of the lockdown measure are important in minimizing the burden of the COVID-19 pandemic in India.

## 6. Discussion and concluding remarks

As the COVID-19 pandemic emerged in late 2019 and started crippling health systems and economies around the world, governments of various countries were confronted with deciding on which NPI to implement in order to strike a balance between reducing the burden of the pandemic (e.g., reducing the transmission of the disease and consequently the number of hospitalizations and deaths), while not over running down their economies. Irrespective of the choice of intervention measure, human decision (at the individual and community level) has a direct impact on the success of the measure as it can influence the outbreak size and duration of the pandemic. In this study, we developed a hybrid epidemiological-evolutionary game theory model to assess the impact of human response to social-isolation (i.e., SQ and SD) on the evolution of the COVID-19 pandemic burden. The model is set up such that an individual can choose to SQ (at home or at a designated quarantine facility), or social-distance (by avoiding crowds, maintaining a distance of 2 meters from others, respecting community shelter-in-place and lockdown measures, using a face mask in public, etc.), or opt not to adopt any of these NPIs. A cost (that an individual must pay) is associated with choosing each of these three strategies. While SD reduces disease transmission, SQ helps in depleting the susceptible population, and hence reduces the disease burden by reducing the available population to be infected.

We computed the reproduction number of the model and used the expression to assess the impact of SD on containing the pandemic. Parameters like the efficacy of SD, and the detection rate of exposed asymptotically infectious individuals play crucial roles in reducing the basic reproduction number. Our analysis indicates that for a substantial reduction in disease burden and possible elimination, both the efficacy of SD and the proportion of individuals who choose to social-distance should be high and that containing the pandemic will be impossible for moderately efficacious SD even if high SD is combined with high exposed and asymptotically infectious case detection. The numerical value of the basic reproduction number computed using both parameters from the literature and the estimated parameter values using data from India fall within the range of reported basic reproduction numbers for COVID-19 (Hellewell et al., 2020; Ngonghala et al., 2020a,b).

We carried out numerical simulations to assess the impact of human behavior-related parameters on the burden of COVID-19 (measured in terms of the daily number of cases). Our results show a strong dependence between the number of daily cases

of COVID-19, behavioral parameters, and COVID-19 transmission potential. Both SD and SQ of suspected disease cases have been widely used for controlling respiratory infections for a long time (Cetron and Simone, 2004; Goh et al., 2006; Ngonghala et al., 2020). Our study shows that SD is more effective in mitigating the burden of the COVID-19 pandemic than SQ. This is due to the fact that SD limits the transmission rate by reducing the number of effective contacts in the population, while SQ reduces the number of new infections by depleting the susceptible pool. It should be mentioned that SD reduces the size of the peak of the pandemic and also delays the time at which the peak occurs, thereby protecting healthcare systems from being overwhelmed, while pharmaceutical interventions, e.g., antiviral drugs and vaccines, are being developed. Individuals opt for SD over SQ, if the perceived cost of the strategy of SD is less than that of SQ. This points to the fact that public health interventions should be directed towards implementing and sustaining SD, as this not only delays the onset of community transmission, but also reduces the cumulative incidence at lower individual cost. This result is consistent with findings in a number of studies including that in Ngonghala et al. (2020), which also highlighted the fact that SD is a better measure for combating COVID-19 than SQ. In advancing these interventions to contain the pandemic, it is important to educate the public on the need to social-distance, and to consider public acceptance of SD measures. This will go a long way to contribute to the success of SD in reducing the burden of the COVID-19 pandemic. On the other hand, during an ongoing pandemic like COVID-19, the flexibility to move and travel without respecting SD strictly is equivalent to acting against important precautionary principles.

While SD and SQ play crucial roles in reducing the burden of COVID-19 (Ferguson et al., 2020), it is important to understand the influence of the perceived efficacy of these two strategies, and the respective impacts of these efficacy on disease dynamics. We account for this by varying the reduced probability of becoming infected, while SD ( $\psi_{sd}$ ) in the range (0,1) and the reduced probability of becoming infected while self-quarantining ( $\psi_{sq}$ ) in the range (0,1). Our results show that ( $\psi_{sd}$ ) has a significant impact on the cumulative incidence of COVID-19, while ( $\psi_{sq}$ ) does not. This suggests that it is more feasible to contain the COVID-19 pandemic by adopting SD compared to SQ. From a public health point of view, SD through community shelter-in-place and mask mandates, avoiding crowded environments, wearing face masks in public, respecting basic personal hygiene, etc., has a huge impact on reducing the spread of the disease. Hence, it is essential to understand the reaction of the public towards SD, and educate individuals and communities on the importance and effectiveness of SD in minimizing the transmission of COVID-19, as well as encourage them to adopt SD.

Our behavior-prevalence model analysis also suggests that the cumulative incidence of the disease decreases with increasing sampling rate, i.e., the rate at which individuals sample others choices before deciding whether to adopt a choice (Fig. 5(b)). Thus, more sampling can bring down the burden of COVID-19. The public health implication of this result is that widespread media coverage on COVID-19 control and mitigation strategies can educate and influence more people to adopt the right strategy.

Due to the absence of safe and effective vaccines or treatments for COVID-19 by the time this study was carried out, SD and SQ were two important NPIs that the governments of many countries used to reduce the burden of the COVID-19 pandemic. These measures played a critical role in delaying the time at which the pandemic will peak ("flatten the epidemic curve") in many countries. This is important in preventing healthcare systems from becoming overwhelmed or overcrowded, while allowing time for governments and health care providers to put together the required resources for fighting the pandemic, or for pharmaceutical companies to develop vaccines and antiviral drugs. Thus, the timing of these measures is very important. For example, China was able to manage the pandemic more effectively because of its early and rapid implementation of such measures (Silva, 2020). Studies in Ngonghala et al. (2020a,b) have also suggested that early implementation of NPIs including SD and mask-use in public is effective in reducing the burden of the COVID-19 pandemic. However, whether these measures are implemented voluntarily by individuals or mandated by government plays a major role in the success of these measures in mitigating the burden of the pandemic. Our study indicates that sequentially switching between voluntary and mandatory implementation of lockdown is a better approach in combating COVID-19 compared to implementing only voluntary or only mandatory social-isolation. This will contribute to minimizing the number of daily cases and also save the country from substantial economic depression. However, optimality of a sequential voluntary vs. mandatory approach will be based on when it was implemented and the stringency condition. Overall, our simulations suggest that a combination of *Mandatory-Voluntary* approach of social-isolation may be useful for reducing disease transmission and for decreasing the cumulative incidence depending on the type of intervention, when, and for how long the measure was implemented.

To validate our model and execute a scenario analysis, we trained the model system with various data sets (e.g., COVID-19 incidence data, information on lockdown, the perceived probability of infection, government stringency condition, etc.) that pertain to India. Through an interactive approach, we estimated values for some of the behavioral and COVID-19 transmission parameters. The estimated parameter values suggest that the relative proportion of asymptotically infectious individuals accounts for higher COVID-19 transmission than symptomatically infectious individuals in India. This is in line with results in Moghadas et al. (2020), Ngonghala et al. (2020), Tindale et al. (2020). This comes as no surprise, since the asymptomatic infectious individuals are not clinically ill and so they mingle freely with others in the community as opposed to the clinically sick, i.e., the symptomatically infectious, who are self-isolating or isolated at hospitals or other designated facilities. We performed several scenario analyses, e.g., extending the period of strict lockdown, initiating the lockdown mandate early, and relaxing strict lockdown measures. The analysis indicates that mandatory strict lockdown is useful in reducing COVID-19 transmission in India. However, an optimal design of lockdown measures that takes into account the type of lockdown, initiation of lockdown, and the duration of the lockdown measure is important in minimizing the burden of the COVID-19 pandemic in India.

A number of simplifying assumptions were considered in deriving the epidemiological and behavior models (1) and (5), respec-

tively. For the epidemiological model, demographic processes (vital dynamics), i.e., births, deaths, or migrations, are excluded from the dynamics, which is realistic for a new disease such as COVID-19 since the time scale of the disease is shorter than that of human demographic processes. Also, a homogeneously mixing population is considered, i.e., any individual in the population has the same chance or probability of interacting with any other individual in the population. However, it should be mentioned that accounting for heterogeneities such as age-structure, preferential mixing, risk structure (e.g., with or without pre-existing health conditions), socio-economic status of individuals and sub-populations, etc., might alter the results described in this paper. Additionally, it is assumed that the time spent in each compartmental class is exponentially-distributed. Furthermore, it is assumed that COVID-19 confers long-lasting immunity against re-infection, i.e., individuals who have acquired COVID-19 and recovered from it acquire natural protective immunity from the disease. It should be mentioned that there is currently not enough data to determine the level and duration of natural immunity to COVID-19. For the behavioral component of the model (7), it is assumed that the risk profile for a specific behavior is the same for all age groups, which is not realistic in general. An age-specific modelling framework may be more suitable to consider since not only different disease transmission probabilities will be accounted for, but also variable risk profiles for different age groups.

In addition to the above limitations, further extensions to the framework described here include accounting for the socio-economic impact of COVID-19 on various populations. To this effect, a coupled COVID-19-human behavior-economic model is under study and will be reported in a separate manuscript. With the availability of highly efficacious vaccines against COVID-19, and with the scepticism surrounding human choice to accept to be vaccinated or not, it is important to consider the impact of this vaccine and human choice on the COVID-19 pandemic. On the other hand, the risk perception and decision-making towards SQ or SD relates to an individual's age and culture (Kim and Crimmins, 2020), e.g., an older person might prefer SQ, while a teenager might opt for nothing or at best SD. This age-dependent variability in decision-making among individuals will create heterogeneity in the model structure and can result in interesting dynamics and more realistic predictions. Additionally, methods described in Glennan (2005), Wu et al. (2013) and Chang et al. (2020) can be used to distinguish between behavioral and mechanical adequacy of the mechanisms represented by the model and to analyze the robustness of the model outcomes through a sensitivity analysis, which distinguishes robustness of the model from the robustness of the model outcomes.

#### CRediT authorship contribution statement

**Calistus N. Ngonghala:** Conceptualization, Formal analysis, Data curation, Investigation, Methodology, Visualization, Writing - original draft, Writing - review & editing. **Palak Goel:** Formal analysis, Data curation, Writing - original draft. **Daniel Kutor:** Formal Analysis. **Samit Bhattacharyya:** Conceptualization, Formal analysis, Data curation, Investigation, Methodology, Validation, Writing - original draft, Writing - review & editing.

#### Declaration of Competing Interest

The authors declare that they have no known competing financial interests or personal relationships that could have appeared to influence the work reported in this paper.

## Acknowledgement

CNN acknowledges the support of the Simons Foundation (Award #627346). The authors thank Prof. Abba B. Gumel (from Arizona State University) for reading through the first draft of the manuscript and providing valuable comments. All authors are thankful to the reviewers and editor for their valuable comments and suggestions to improve the analysis and presentation. Also, the authors express their deepest sympathy to the families of the victims of SARS-CoV-2, and extend profound appreciation to the frontline healthcare workers for their heroic efforts and sacrifices to save the lives of others.

## Appendix A. Supplementary data

Supplementary data associated with this article can be found, in the online version, at <https://doi.org/10.1016/j.jtbi.2021.110692>.

## References

- Acemoglu, D., Chernozhukov, V., Werning, I., Whinston, M.D., 2020. A multi-risk SIR model with optimally targeted lockdown. Technical Report, National Bureau of Economic Research.
- Alvarez, F.E., Argente, D., Lippi, F., 2020. A simple planning problem for covid-19 lockdown. Technical Report, National Bureau of Economic Research.
- Bauch, C.T., 2005. Imitation dynamics predict vaccinating behaviour. *Proceedings of the Royal Society B: Biological Sciences* 272 (1573), 1669–1675.
- Bhattacharyya, S., Bauch, C., 2010. A game dynamic model for delayer strategies in vaccinating behaviour for pediatric infectious diseases. *Journal of Theoretical Biology* 267 (3), 276–282.
- Blower, S.M., Dowlatbadi, H., 1994. Sensitivity and uncertainty analysis of complex models of disease transmission: an HIV model, as an example. *International Statistical Review/Revue Internationale de Statistique* 62 (2), 229–243.
- Briz-Redón, Á., Serrano-Aroca, Á., 2020. A spatio-temporal analysis for exploring the effect of temperature on COVID-19 early evolution in Spain. *Science of the Total Environment* 138811.
- Brooks, S.K., Webster, R.K., Smith, L.E., Woodland, L., Wessely, S., Greenberg, N., Rubin, G.J., 2020. The psychological impact of quarantine and how to reduce it: rapid review of the evidence. *The Lancet* 395 (10227), 912–920.
- Brotherhood, L., Kircher, P., Santos, C., Tertilt, M., 2020. An economic model of the COVID-19 epidemic: The importance of testing and age-specific policies..
- Cetron, M., Simone, P., 2004. Battling 21<sup>st</sup>-century scourges with a 14<sup>th</sup>-century toolbox. *Emerging Infectious Diseases* 10 (11), 2053.
- Chang, S.L., Harding, N., Zachreson, C., Cliff, O.M., Prokopenko, M., 2020. Modelling transmission and control of the COVID-19 pandemic in Australia. *Nature Communications* 11 (1), 5710. <https://doi.org/10.1038/s41467-020-19393-6>.
- Chudik, A., Pesaran, M.H., Rebucci, A., 2020. Voluntary and mandatory social distancing: Evidence on COVID-19 exposure rates from Chinese provinces and selected countries. Technical Report, National Bureau of Economic Research.
- Dickens, B.L., Koo, J.R., Lim, J.T., Park, M., Quaye, S., Sun, H., Sun, Y., Pung, R., Wilder-Smith, A., Chai, L.Y.A., et al., 2020. Modelling lockdown and exit strategies for COVID-19 in Singapore. *The Lancet Regional Health-Western Pacific* 1, 100004.
- Diekmann, O., Heesterbeek, J.A.P., Metz, J.A., 1990. On the definition and the computation of the basic reproduction ratio  $R_0$  in models for infectious diseases in heterogeneous populations. *Journal of Mathematical Biology* 28 (4), 365–382.
- Dong, E., Du, H., Gardner, L. Coronavirus COVID-19 Global Cases by Johns Hopkins CSSE, *The Lancet Infectious Diseases*, 2020. URL: <https://gisanddata.maps.arcgis.com/apps/opsdashboard/index.html#/bda7594740fd40299423467b48e9ecf6>.
- Dong, E., Du, H., Gardner, L., 2020. An interactive web-based dashboard to track covid-19 in real time. *The Lancet Infectious Diseases* 20 (5), 533–534.
- European Centre for Disease Prevention and Control, 2020. Considerations relating to social distancing measures in response to covid-19: second update. URL: <https://www.ecdc.europa.eu/en/publications-data/considerations-relating-social-distancing-measures-response-covid-19-second>.
- Farboodi, M., Jarosch, G., Shimer, R., 2020. Internal and external effects of social distancing in a pandemic. Technical Report, National Bureau of Economic Research.
- Ferguson, N.M., Laydon, D., Nedjati-Gilani, G., Imai, N., Ainslie, K., Baguelin, M., et al., 2020. Imperial college COVID-19 Response Team. Impact of non-pharmaceutical interventions (NPIs) to reduce COVID-19 mortality and healthcare demand. Published March 16, 2020..
- Ferguson, N.M., Laydon, D., Nedjati-Gilani, G., Imai, N., Ainslie, K., Baguelin, M., et al., 2020. Imperial college COVID-19 response team. Impact of non-pharmaceutical interventions (NPIs) to reduce COVID-19 mortality and healthcare demand. Published March 16, 2020..
- Flaxman, S., Mishra, S., Gandy, A., Unwin, H.J.T., Mellan, T.A., Coupland, H., Whittaker, C., Zhu, H., Berah, T., Eaton, J.W., et al., 2020. Estimating the effects of non-pharmaceutical interventions on COVID-19 in Europe. *Nature* 584 (7820), 257–261.
- Gatto, M., Bertuzzo, E., Mari, L., Miccoli, S., Carraro, L., Casagrandi, R., Rinaldo, A., 2020. Spread and dynamics of the COVID-19 epidemic in Italy: Effects of emergency containment measures. *Proceedings of the National Academy of Sciences* 117 (19), 10484–10491.
- Gelfand, M., Jackson, J.C., Pan, X., Nau, D., Dagher, M., Chiu, C.-Y., 2020. Cultural and institutional factors predicting the infection rate and mortality likelihood of the COVID-19 pandemic. *PsyArXiv*.
- Germani, A., Buratta, L., Delvecchio, E., Mazzeschi, C., 2020. Emerging adults and covid-19: The role of individualism-collectivism on perceived risks and psychological maladjustment. *International Journal of Environmental Research and Public Health* 17 (10), 3497.
- Gettleman, J., 2020. As virus infections surge, countries end lockdowns, *The New York Times*. URL: <https://www.nytimes.com/2020/06/10/world/asia/reopening-before-coronavirus-ends.html>.
- Giuliani, D., Dickson, M.M., Espa, G., Santi, F., 2020. Modelling and predicting the spatio-temporal spread of coronavirus disease 2019 (COVID-19) in Italy. Available at SSRN 3559569..
- Glennan, S., 2005. Modeling mechanisms. *Studies in History and Philosophy of Science Part C: Studies in History and Philosophy of Biological and Biomedical Sciences* 36 (2), 443–464.
- Goh, K.-T., Cutter, J., Heng, B.-H., Ma, S., Koh, B.K., Kwok, C., Toh, C.-M., Chew, S.-K., 2006. Epidemiology and control of SARS in Singapore. *Annals-Academy of Medicine Singapore* 35 (5), 301.
- Gonzalez-Eiras, M., Niepelt, D., 2020. On the optimal lockdown during an epidemic. Technical Report, CESifo working paper.
- Gumel, A.B., Iboi, E.A., Ngonghala, C.N., Elbasha, E.H., 2021. A primer on using mathematics to understand covid-19 dynamics: Modeling, analysis and simulations. *Infectious Disease Modelling* 6, 148–168.
- Gumel, A.B., Iboi, E.A., Ngonghala, C.N., Ngwa, G.A., 2021. Towards achieving a vaccine-derived herd immunity threshold for COVID-19 in the U.S., *medRxiv*.
- Hellewell, J., Abbott, S., Gimma, A., Bosse, N.I., Jarvis, C.I., Russell, T.W., Munday, J.D., Kucharski, A.J., Edmunds, W.J., Sun, F., et al., 2020. Feasibility of controlling COVID-19 outbreaks by isolation of cases and contacts. *The Lancet Global Health* 8 (4), e488–e496.
- Iboi, E.A., Ngonghala, C.N., Gumel, A.B., 2020. Will an imperfect vaccine curtail the COVID-19 pandemic in the U.S.? *Infectious Disease Modelling* 5, 510–524.
- Jones, C.J., Philippon, T., Venkateswaran, V., 2020. Optimal mitigation policies in a pandemic: Social distancing and working from home. Technical Report, National Bureau of Economic Research.
- Institute for Health Metrics and Evaluation, 2020. COVID-19 health service utilization forecasting team. Forecasting COVID-19 impact on hospital bed-days, ICU-days, ventilator-days and deaths by us state in the next 4 months, *medRxiv*.
- Kang, D., Choi, H., Kim, J.-H., Choi, J., 2020. Spatial epidemic dynamics of the COVID-19 outbreak in China. *International Journal of Infectious Diseases* 94, 96–102.
- Karaye, I.M., Horney, J.A., 2020. The impact of social vulnerability on COVID-19 in the U.S.: an analysis of spatially varying relationships. *American Journal of Preventive Medicine* 59 (3), 317–325.
- Kim, J.K., Crimmins, E.M., 2020. How does age affect personal and social reactions to COVID-19: Results from the national understanding America study. *PLoS One* 15 (11), e0241950.
- Maier, B.F., Brockmann, D., 2020. Effective containment explains subexponential growth in recent confirmed COVID-19 cases in China. *Science* 368 (6492), 742–746.
- Marino, S., Hogue, I.B., Ray, C.J., Kirschner, D.E., 2008. A methodology for performing global uncertainty and sensitivity analysis in systems biology. *Journal of Theoretical Biology* 254 (1), 178–196.
- Martellucci, C.A., Sah, R., Rabaan, A.A., Dhama, K., Casalone, C., Arteaga-Livias, K., Sawano, T., Ozaki, A., Bhandari, D., Higuchi, A., et al., 2020. Changes in the spatial distribution of COVID-19 incidence in Italy using GIS-based maps. *Annals of Clinical Microbiology and Antimicrobials* 19 (1), 1–4.
- McKay, M.D., Beckman, R.J., Conover, W.J., 2000. A comparison of three methods for selecting values of input variables in the analysis of output from a computer code. *Technometrics* 42 (1), 55–61.
- Moghadas, S.M., Fitzpatrick, M.C., Sah, P., Pandey, A., Shoukat, A., Singer, B.H., Galvani, A.P., 2020. The implications of silent transmission for the control of COVID-19 outbreaks. *Proceedings of the National Academy of Sciences* 117 (30), 17513–17515.
- Mollalo, A., Vahedi, B., Rivera, K.M., 2020. GIS-based spatial modeling of COVID-19 incidence rate in the continental United States. *Science of The Total Environment* 728, 138884.
- Max Roser, E.O.-O., Ritchie, Hannah, Hasell, J., 2020. Coronavirus pandemic (COVID-19). *Our World in Data*. URL: <https://ourworldindata.org/coronavirus>.
- Ngonghala, C.N., Iboi, E., Eikenberry, S., Scotch, M., MacIntyre, C.R., Bonds, M.H., Gumel, A.B., 2020. Mathematical assessment of the impact of non-pharmaceutical interventions on curtailing the novel coronavirus. *Mathematical Biosciences* 325, 108364.
- Ngonghala, C.N., Iboi, E.A., Gumel, A.B., 2020. Could masks curtail the post-lockdown resurgence of COVID-19 in the U.S.? *Mathematical Biosciences* 329, 108452.
- Pindyck, R.S., 2020. COVID-19 and the welfare effects of reducing contagion. Technical Report, National Bureau of Economic Research.
- Routley, N., 2020. Where COVID-19 is rising and falling around the world, *HealthCare*. URL: <https://www.visualcapitalist.com/where-covid-19-is-rising-and-falling-around-the-world/>.

- Shi, P., Dong, Y., Yan, H., Zhao, C., Li, X., Liu, W., He, M., Tang, S., Xi, S., 2020. Impact of temperature on the dynamics of the COVID-19 outbreak in China. *Science of the Total Environment* 728, 138890.
- Silva, A.A.M.d., 2020. On the possibility of interrupting the coronavirus (COVID-19) epidemic based on the best available scientific evidence. *SciELO Public Health*.
- Travaglino, G.A., Moon, C., 2020. Explaining compliance with social distancing norms during the COVID-19 pandemic: The roles of cultural orientations, trust and self-conscious emotions in the U.S., Italy, and South Korea.
- Tindale, L.C., Stockdale, J.E., Coombe, M., Garlock, E.S., Lau, W.Y.V., Saraswat, M., Zhang, L., Chen, D., Wallinga, J., Colijn, C., 2020. Evidence for transmission of COVID-19 prior to symptom onset. *eLife* 9, e57149.
- Toxvaerd, F., 2020. Equilibrium social distancing. URL: <https://www.repository.cam.ac.uk/handle/1810/305407>.
- Tuite, A.R., Fisman, D.N., Greer, A.L., 2020. Mathematical modelling of COVID-19 transmission and mitigation strategies in the population of Ontario, Canada. *Canadian Medical Association Journal* 192 (19), E497–E505.
- van den Driessche, P., Watmough, J., 2002. Reproduction numbers and sub-threshold endemic equilibria for compartmental models of disease transmission. *Mathematical Biosciences* 180 (1–2), 29–48.
- Walker, P.G., Whittaker, C., Watson, O.J., Baguelin, M., Winskill, P., Hamlet, A., Djafaara, B.A., Cucunubá, Z., Mesa, D.O., Whittaker, C., Watson, O.J., Baguelin, M., Winskill, P., Hamlet, A., Djafaara, B.A., Cucunubá, Z., Mesa, D.O., Green, W., Thompson, H., 2020. The impact of COVID-19 and strategies for mitigation and suppression in low- and middle-income countries. *Science* 369 (6502), 413–422.
- World Health Organization, 2020. Emergencies, preparedness, response. Pneumonia of unknown origin – China, Disease Outbreak News. URL: <https://www.who.int/csr/don/05-january-2020-pneumonia-of-unknown-cause-china/en/>.
- Worldometer, 2020. COVID-19 coronavirus pandemic: reported cases and deaths by country, territory, or conveyance, Worldometer. URL: <https://www.worldometers.info/coronavirus/>.
- World Health Organization, 2020. Coronavirus disease (COVID-2019) Situation Reports, WHO. URL: [https://www.who.int/docs/default-source/coronaviruse/situation-reports/20200417-sitrep-88-covid-191b6cccd94f8b4f219377bff55719a6ed.pdf?sfvrsn=ebe78315\\_6](https://www.who.int/docs/default-source/coronaviruse/situation-reports/20200417-sitrep-88-covid-191b6cccd94f8b4f219377bff55719a6ed.pdf?sfvrsn=ebe78315_6).
- World Health Organization, 2020. Coronavirus disease (COVID-2019) situation dashboard, WHO. URL: <https://covid19.who.int/region/amro/country/us>.
- Wu, J., Dhingra, R., Gambhir, M., Remais, J.V., 2013. Sensitivity analysis of infectious disease models: methods, advances and their application. *Journal of The Royal Society Interface* 10 (86), 20121018.
- Xie, J., Zhu, Y., 2020. Association between ambient temperature and COVID-19 infection in 122 cities from China. *Science of the Total Environment* 724, 138201.
- Yin, Y., Wunderink, R.G., 2018. MERS: SARS and other coronaviruses as causes of pneumonia. *Respirology* 23 (2), 130–137.